Supplementary Material

Text S1. Positive Matrix Factorization (PMF) Analysis.

The PMF version 5.0 (PMF 5.0) was applied to develop source apportionments of organic acids in rainfall events. Seventeen chemical components were used as the model inputs, including inorganic ions (Na^+, NH_4^+, K^+, Mg^+, Ca^{2+}, F^-, Cl^-, NO_2^-, Br^-, NO_3^- and SO_4^{2-}) and organic acids (formic, acetic, MSA, succinic, glutaric, oxalic acid).

We ran the PMF model with 4–9 factors and changed the seed value from 1 to 40. Moreover, we examined the Q (robust) and Q (true) values as well as the number of scaled residuals beyond three standard deviations to select the optimal number of factors. The uncertainties of the PMF solutions for each test run were estimated using the analyses of displacement (DISP) and bootstrap (BS) [1, 2].

The PMF analysis resulted in six interpretable factors, as shown in Figure S8. Factor 1 (F1) was dominated by sodium (90.2%) and chloride (81.9%). Shanghai is a coastal city, and the sea breeze has a great impact on the rain. Therefore, F1 is referred to as "marine source" [3]. Factor 2 (F2) is characterized by the dominance of nitrate (54.4%) and formic acid (85.6%), the source of formic acid is known to be photochemical reaction generation according to previous studies [4]. Thus, F2 is referred to here as "vehicle exhaust and secondary emission source". Factor 3 (F3) is characterized by large contributions of ammonium (61.3%) and sulfate (66.6%). Which may be related to photochemical reactions in the atmosphere [5]. F3 is defined as "secondary sulfate source". Factor 4 (F4) is characterized by acetic acid (73.1%), which is an organic matter emitted by plants [6, 7]. Therefore, F4 is referred to as "biological emission source". Factor 5 (F5) is dominated by potassium (59.2%), which is the main substance produced by biomass combustion [8]. Thus, F5 is referred to here as "biomass combustion source". Factor 6 (F6) is dominated by calcium (80.9%), which is the main component of ground dust. Therefore, F6 is referred to here as "dust source" [9].

Table S1. The rainfall events with corresponding ranges and mean of pH values.

Rainfall Sequences	Dates	Ranges of pH values	Means of pH Values
1	August 2020	5.71—6.33	6.13
2	August 2020	5.11—6.44	5.71
3	August 2020	5.2—5.56	5.4
4	August 2020	5.06—5.85	5.3
5	August 2020	4.61—5.31	4.96
6	August 2020	4.83—4.96	4.87
7	August 2020	4.2—4.6	4.39
8	September 2020	6.16—6.68	6.51
9	September 2020	4.97—6.59	5.39
10	September 2020	4.42—4.78	4.64
11	September 2020	4.96—5.49	5.34
12	September 2020	5.76—6.25	6.03
13	September 2020	3.95—5.09	4.22
14	September 2020	3.99—4.88	4.28
15	September 2020	4.91—5.22	5.12
16	September 2020	4.87—5.35	5.18
17	September 2020	5.22—5.33	5.25
18	September 2020	3.95—4.96	4.24
19	September 2020	4.32—4.87	4.54
20	September 2020	5.01—5.15	5.08
21	September 2020	4.11—4.65	4.31
22	September 2020	4.81—5.15	4.95
23	September 2020	4.41—4.71	4.56
24	September 2020	5.71—6.42	6.11
25	September 2020	4.82—5.43	4.97
26	September 2020	4.95—5.53	5.24
27	October 2020	4.14—4.54	4.27
28	October 2020	5.45—7.01	6.06
29	October 2020	5.53—6.51	6.09
30	November 2020	4.3—4.97	4.79
31	November 2020	4.58—4.92	4.75
32	November 2020	4.89—5.35	5.05
33	November 2020	5.15—5.59	5.37
34	November 2020	4.42—6.29	5.24
35	November 2020	6.32—6.49	6.44
36	November 2020	4.45—5.93	5
37	November 2020	4.35—5.09	4.61
38	December 2020	7.05—7.15	7.1

39	December 2020	6.76—6.94	6.79
40	December 2020	6.32—7.52	7.14
41	January 2021	4.84—7.37	5.74
42	January 2021	4.4—5.79	4.76
43	January 2021	7.01—7.29	7.13
44	February 2021	4.76—5.36	5.01
45	February 2021	4.56—6.42	5.37
46	February 2021	4.49—5.09	4.61
47	February 2021	4.59—5.49	5.08
48	March 2021	4.4—4.85	4.62
49	March 2021	4.63—5.36	5.02
50	March 2021	6.89—7.26	7.1
51	March 2021	7.19—7.26	7.23
52	March 2021	6.89—7.22	7.02
53	March 2021	5.39—6.7	5.83
54	March 2021	4.23—6.36	4.57
55	March 2021	4.27—5.81	4.64
56	March 2021	4.61—6.66	5.03
57	March 2021	4.64—6.62	5.19
58	April 2021	6.11—7.02	6.59
59	April 2021	5.04—6.82	5.69
60	April 2021	5.28—5.33	5.29
61	April 2021	4.91—5.48	5.29

Table S2. Correlation analysis of organic acids and inorganic ions.

	T	pH	EC	Na^+	NH_4^+	K^+	Mg^+	Ca^{2+}	F^-	Acetic	Formic	MSA	Cl^-	NO_2^-	NO_3^-	Glutaric	Succinic	SO_4^{2-}	Oxalic
T	1																		
pH	-0.336**	1																	
EC	-0.132**	0.083*	1																
Na^+	-0.125**	0.267**	0.556**	1															
NH_4^+	-0.307**	0.237**	0.591**	0.245**	1														
K^+	-0.211**	0.394**	0.486**	0.534**	0.482**	1													
Mg^+	-0.132**	0.326**	0.667**	0.908**	0.423**	0.694**	1												
Ca^{2+}	-0.110**	0.504**	0.615**	0.624**	0.481**	0.679**	0.806**	1											
F^-	-0.083*	0.239**	0.465**	0.341**	0.431**	0.465**	0.502**	0.592**	1										
Acetic	0.039	0.020	0.358**	0.124**	0.538**	0.277**	0.308**	0.403**	0.457**	1									
Formic	0.129**	-0.017	0.387**	0.059	0.463**	0.256**	0.254**	0.374**	0.286**	0.758**	1								
MSA	-0.078	0.132**	0.359**	0.240**	0.406**	0.289**	0.299**	0.289**	0.172**	0.312**	0.382**	1							
C^-	-0.132**	0.256**	0.535**	0.911**	0.282**	0.506**	0.872**	0.573**	0.343**	0.137**	0.114**	0.286**	1						
NO_2^-	-0.223**	0.523**	0.265**	0.229**	0.499**	0.433**	0.313**	0.459**	0.245**	0.273**	0.143**	0.217**	0.209**	1					
NO_3^-	0.033	0.080*	0.712**	0.517**	0.642**	0.451**	0.687**	0.723**	0.503**	0.525**	0.552**	0.378**	0.559**	0.248**	1				
Glutaric	-0.036	0.042	0.373**	0.318**	0.422**	0.319**	0.421**	0.386**	0.277**	0.417**	0.465**	0.302**	0.383**	0.120**	0.513**	1			
Succinic	-0.015	0.046	0.438**	0.228**	0.461**	0.380**	0.386**	0.459**	0.323**	0.560**	0.685**	0.279**	0.312**	0.164**	0.592**	0.617**	1		
SO_4^{2-}	-0.299**	0.216**	0.652**	0.545**	0.738**	0.574**	0.662**	0.613**	0.439**	0.387**	0.337**	0.456**	0.648**	0.368**	0.699**	0.507**	0.564**	1	
Oxalic	-0.281**	0.146**	0.517**	0.429**	0.561**	0.482**	0.532**	0.491**	0.377**	0.389**	0.469**	0.307**	0.438**	0.124**	0.531**	0.575**	0.638**	0.698**	1

Note: ** represents "$p < 0.01$", * represents "$p < 0.05$"
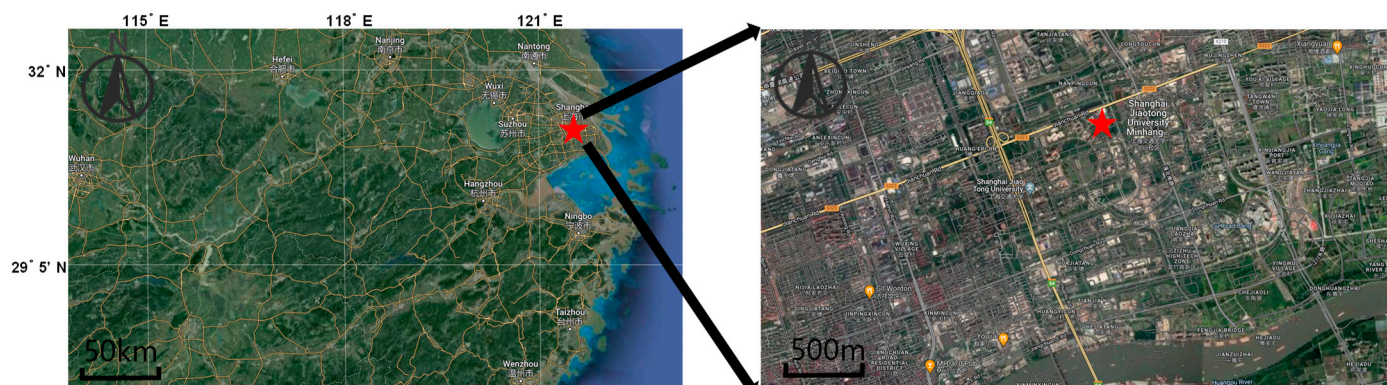
Figure S1. Map showing the location of the sampling site and its surrounding.

Figure S2. Automatic volume-based sequential rain sampler

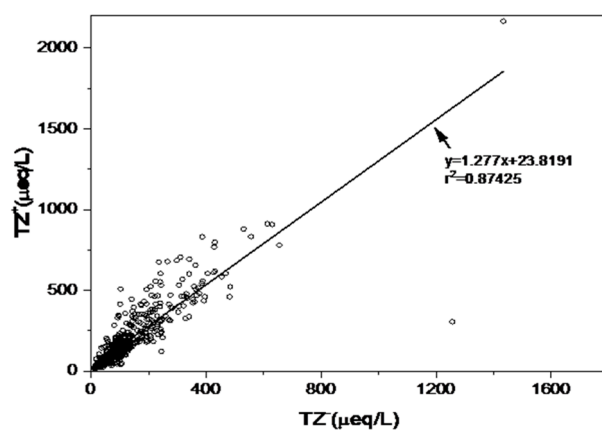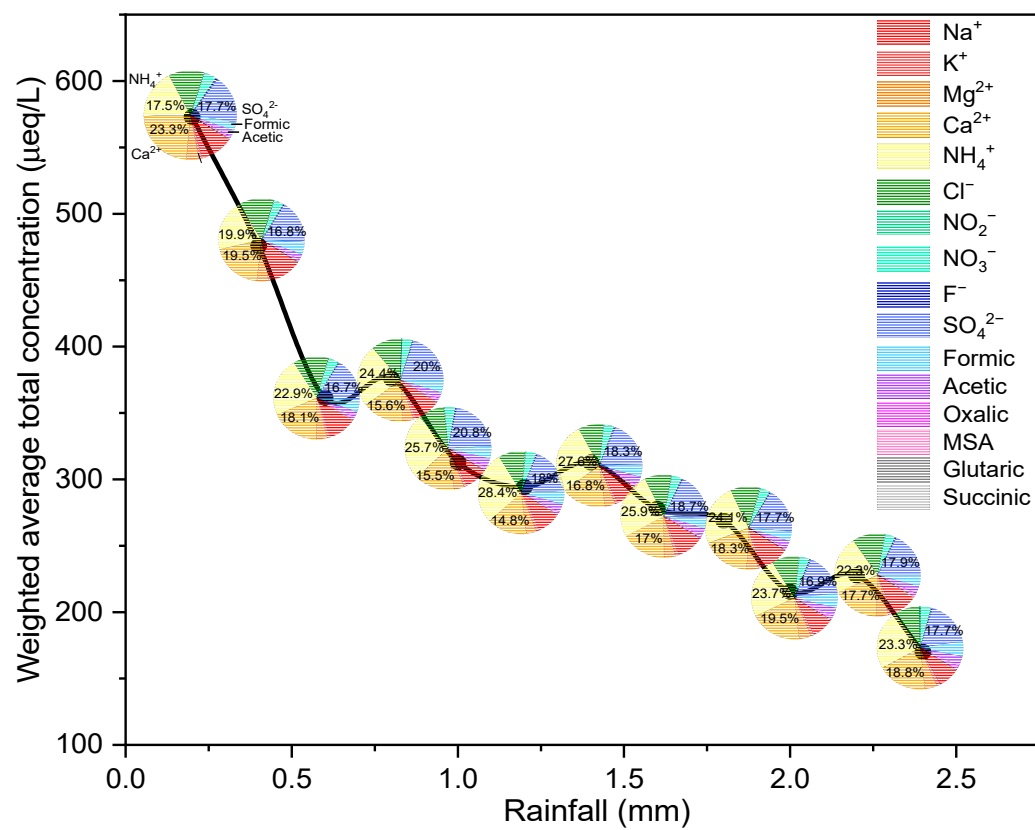**Figure S3.** Ion balance between total cations (TZ$^+$) and total anions (TZ$^-$)

Figure S4. The proportions of ion concentration in rainfall events change with rainfall. The cumulative rainfall is taken as the abscissa and the total ion concentration as the ordinate. Each pie chart represents the concentration proportions of the corresponding cumulative rainfall.

Figure S5. Concentration comparisons of inorganic ions and organic acids in early sequences of rainfall events and cloud water. **(a)** Concentration comparisons of inorganic ions in early sequences of rainfall events and cloud water. **(b)** Concentration comparisons of organic acids in early sequences of rainfall events and cloud water. The upper half-circle represents cloud water. The lower circle represents early sequences of rainfall events.
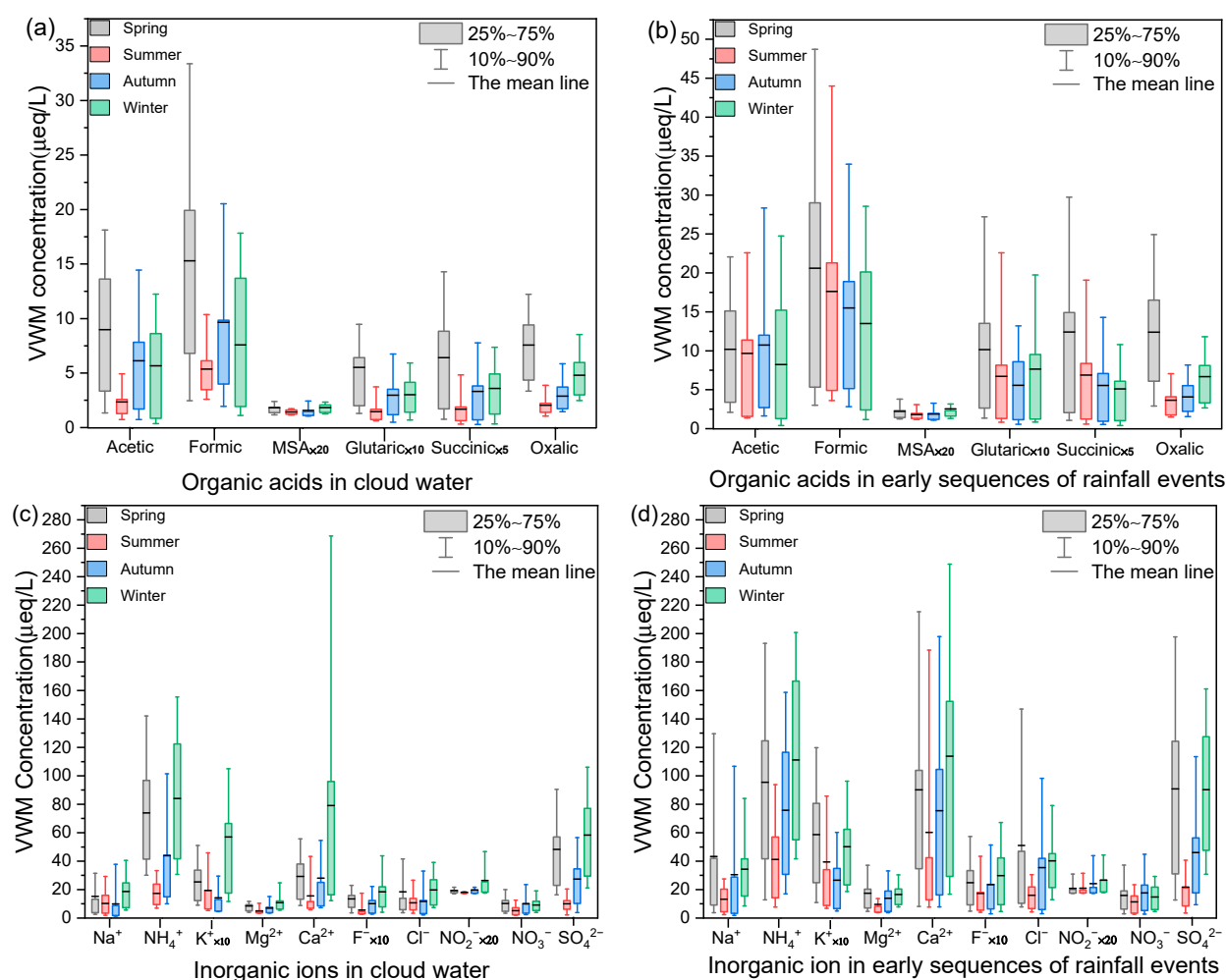
Figure S6. Seasonal concentration variations of organic acids and inorganic ions in early sequences of rainfall events and cloud water. (a) Seasonal concentration variations of organic acids in cloud water. (b) Seasonal concentration variations of organic acids in early sequences of rainfall events. (c) Seasonal concentration variations of inorganic ions in cloud water. (d) Seasonal concentration variations of inorganic ions in early sequences of rainfall events.

References

1. Muller, A., Y. Miyazaki, E. Tachibana, K. Kawamura, and T. Hiura. "Evidence of a Reduction in Cloud Condensation Nuclei Activity of Water-Soluble Aerosols Caused by Biogenic Emissions in a Cool-Temperate Forest." Scientific Reports 7 (2017).doi:https://doi.org/10.1038/s41598-017-08112-9.
2. Brown, S. G., S. Eberly, P. Paatero, and G. A. Norris. "Methods for Estimating Uncertainty in Pmf Solutions: Examples with Ambient Air and Water Quality Data and Guidance on Reporting Pmf Results." Science of the Total Environment 518 (2015): 626-35.doi:https://doi.org/10.1016/j.scitotenv.2015.01.022.
3. Wang, Qiongzhen, Guoshun Zhuang, Kan Huang, Tingna Liu, Congrui Deng, Jian Xu, Yanfen Lin, Zhigang Guo, Ying Chen, Qingyan Fu, Joshua S. Fu, and Jiakuan Chen. "Probing the Severe Haze Pollution in Three Typical Regions of China: Characteristics, Sources and Regional Impacts." Atmospheric environment. 120, no. Nov. (2015): 76-88.doi:https://doi.org/10.1016/j.atmosenv.2015.08.076.
4. Meng, Ya, Yilong Zhao, Rui Li, Junlin Li, Lulu Cui, Lingdong Kong, and Hongbo Fu. "Characterization of Inorganic Ions in Rainwater in the Megacity of Shanghai: Spatiotemporal Variations and Source Apportionment." Atmospheric research 222, no. Jul. (2019): 12-24.doi:https://doi.org/10.1016/j.atmosres.2019.01.023.
5. Dentener, Frank J, and Paul J Crutzen. "A Three-Dimensional Model of the Global Ammonia Cycle." Journal of Atmospheric Chemistry 19, no. 4 (1994): 331-69.doi:https://doi.org/10.1007/bf00694492.

6.   Bates.TS, Lamb.BK, Guenther.A, Dignon.J, and Stoiber.RE. "Sulfur Emissions to the Atmosphere from Natural Sourees." Journal of Atmospheric Chemistry 14, no. 1 (1992): 315-37.doi:https://doi.org/10.1007/bf00115242.

7.   Kerminen, VELI-MATTI, MINNA AURELA, RISTO E. HILLAMO, and AKI VIRKKULA. "Formation of Particulate Msa: Deductions from Size Distribution Measurements in the Finnish Arctic." Tellus B: Chemical and Physical Meteorology 49, no. 2 (1997): 159-71.doi:https://doi.org/10.1034/j.1600-0889.49.issue2.4.x.

8.   Lee, Sangil, Wei Liu, Yuhang Wang, Armistead G Russell, and Eric S Edgerton. "Source Apportionment of Pm2. 5: Comparing Pmf and Cmb Results for Four Ambient Monitoring Sites in the Southeastern United States." Atmospheric environment 42, no. 18 (2008): 4126-37.doi:https://doi.org/10.1016/j.atmosenv.2008.01.025.

9.   Li, YunChun, Meng Zhang, Man Shu, Steven Sai Hang Ho, Zi-Fang Liu, Xian-Xiang Wang, and Xiao-Qing Zhao. "Chemical Characteristics of Rainwater in Sichuan Basin, a Case Study of Ya'an." Environmental Science and Pollution Research 23, no. 13 (2016): 13088-99.doi:https://doi.org/10.1007/s11356-016-6363-4.